Journal of Molecular Structure 1139 (2017) 353–361

Contents lists available at ScienceDirect

Journal of Molecular Structure

journal homepage: http://www.elsevier.com/locate/molstruc

Structural study of a novel acetylide-thiourea derivative and its evaluation as a detector of benzene

Wan M. Khairul [a, *], Adibah Izzati Daud [a, b], Noor Azura Mohd Hanifaah [a], Suhana Arshad [c], Ibrahim Abdul Razak [c], Hafiza Mohamed Zuki [d], Mauricio F. Erben [e]

[a] School of Fundamental Science, Universiti Malaysia Terengganu, 21030, Kuala Terengganu, Terengganu, Malaysia
[b] Faculty of Engineering Technology, Universiti Malaysia Perlis (UniMAP), Level 1, Blok S2, Kampus UniCITI Alam, Sungai Chuchuh, Padang Besar, 02100, Perlis, Malaysia
[c] School of Physics, Universiti Sains Malaysia, 11800, USM, Penang, Malaysia
[d] School of Marine Science and Environment, Universiti Malaysia Terengganu, 21030, Kuala Terengganu, Terengganu, Malaysia
[e] CEQUINOR (UNLP, CONICET-CCT La Plata), Departamento de Química, Facultad de Ciencias Exactas, Universidad Nacional de La Plata, C.C. 962 (1900), La Plata, Argentina

ARTICLE INFO

Article history:
Received 26 December 2016
Received in revised form
16 March 2017
Accepted 16 March 2017
Available online 22 March 2017

Keywords:
Acetylide
Thiourea
Spectroscopy
DFT
Synthesis
Crystallography

ABSTRACT

The new derivative 1-hexanoyl-3-(4-*p*-tolylethynyl-phenyl)-thiourea **(APHX)** was synthesised by the addition reaction between 4[4-aminophenyl] ethynyltoluene and hexanoyl isothiocyanate in acetone. The acetylide group was incorporated by using Sonogashira cross-coupling reaction allowing for the preparation of acetylide-thiourea compound. **APHX** was then elucidated via single crystal X-ray crystallography analysis, spectroscopic and elemental analysis by Fourier Transform Infrared (FT-IR) spectroscopy, ^{1}H and ^{13}C Nuclear Magnetic Resonance (NMR), UV–visible analysis, CHNS-elemental analysis. **APHX** was also evaluated theoretically via density functional theory (DFT) approach. **APHX** was fabricated onto glass substrate via drop-cast technique prior to act as optical thin-film and its performance as volatile organic compounds (VOCs) sensor was investigated through the difference in UV–vis profile before and after exposure towards benzene. Preliminary findings revealed that **APHX** showed interaction towards benzene with about 48% sensitivity. According to thermogravimetric studies, **APHX** showed good thermal stability, without decomposition up to *ca.* 190 °C. Whilst, crystal structure of **APHX** consists in a nearly planar acylthiourea moiety with the C=O and C=S bonds utilizing *trans* position, favoring by an intramolecular N–H···O=C hydrogen bonds. The alkyl chain is oriented 90° with respect to acylthiourea group. The phenyls group in the 1-methyl-4-(phenylethynyl)benzene moieties are mutually planar and slightly twisted with respect to the acylthiourea plane. Centrosymmetric dimers generated by intermolecular N–H···S=C and C–H···S=C hydrogen bonds forming $R_2^2(8)$ and $R_2^1(6)$ motifs are present in the crystals. The interaction between **APHX** with benzene has been modelled and calculated using density functional theory (DFT) via Gaussian 09 software package and the preferred sites of binding are located at the acylthiourea group.

1. Introduction

The existence of toxic volatile organic compounds (VOCs) namely toluene, methanol, acetone, and benzene in most workplace environment have resulted the death of many workers who were directly exposed to VOCs over the last century [1]. Benzene particularly is known to be one of the human carcinogenic substances classified as Group A as both acute and chronic health hazard [2–5] on humans depending on VOCs analyte concentration and time of exposure. It can cause serious health effects in human for instance, eye inflammation, headaches, cancer, and other organ damages [6]. Therefore, there are growing demands to develop class of new gas sensors or at least improving the sensing properties of the existing sensing materials [7,8]. Thus, serious efforts have been actively carried out to propose and develop new active sensing materials with enhanced sensing properties, as alternatives to the existing sensing materials with utmost performances in term of sensitivity, selectivity, and reproducibility.

* Corresponding author.
E-mail address: wmkhairul@umt.edu.my (W.M. Khairul).

http://dx.doi.org/10.1016/j.molstruc.2017.03.065
0022-2860/

In previous occasions, VOCs (benzene) analyte has been detected by carbon nanotubes based materials [9,10], conductive polymeric system [11–13], and metal oxides derivatives [14–16], which needs special treatments like large instrumentation, high operating temperature, and inert environment in order to be operated. Indeed, the developments of alternative, robust and well-defined sensing materials for the detection of VOCs have become the subject of demand in current situation. In this work, we introduce the unique ability of acetylide-thiourea derivative to be employed as active sensing material for VOCs detection. This is due to the benefits of using single-molecular based system in which the molecular framework can be easily designed and tuned to be suited with the selected analyte of interest [17]. It also should be able to operate at room temperature under ambient atmosphere, exhibit ease of synthetic work-up and offer ease of deposition method [18] with high chemical stability [19].

Thiourea derivatives are known as versatile ligands which have ability to bind with metal ions in various coordination modes to form stable complexes [20] depending on various factors such as, conformational isomerism, steric effects, the presence of donor chelating site on the substituent groups and intramolecular interaction. Consequently, this fact on thiourea derivatives have gained interest in the complexation properties of carbonyl (C═O) and thiol (C═S) [21]. For instance, thiourea derivatives resulting as substituted benzoylthiourea introducing acetylide (C≡C) moiety is known to be promising compounds in materials chemistry due to their ability in the formation of intra and intermolecular hydrogen bonds of N–H proton donor group to carbonyl oxygen and sulphur atoms which indeed enhanced the electron rich properties in molecular structures [22].

There are increasing interests in the respect of structural and conformational elucidation of hybrid moieties of thiourea derivatives since they are known as a crucial part for acetylide-thiourea derivatives to be developed as chemosensors either as anion recognition [23] or gas detection [24]. In particular, acetylide-thiourea and gases molecules participate in sensing behaviour via van der Waals interaction [25], indeed playing an important role to act as molecular wires exhibited donor-π-acceptor (D-π-A) properties. In fact, it is well-known that the planar structure of C(O)NHC(S)NH moiety, favoured for acyl/aroyl acetylide-thiourea derivatives, with *trans* orientation between C═O and C═S. Thus, a pseudo six-membered ring is occurred in this conformation, related with the formation of a C═O···H–N intramolecular hydrogen bond.

Both, thiourea and acetylide motifs are commonly been widely investigated in various advanced materials applications [26–29]. Important applications are based on their capacity for electronic transport throughout molecular backbone favoured by rigid π-conjugated systems. In addition, the ability of thiourea derivatives to bind with other targeted analytes such as metals [23] or gas molecules [24] via thione (C═S) or carbonyl (C═O) groups make them applicable as molecular sensors. The presence of lone pair electrons in N, O, and S atoms which implicate the resonance effect of electron delocalisation throughout conjugated molecular system which lead to the active molecular system contained rich electron density properties.

In this contribution, a new derivative containing both acetylide and thiourea groups, namely 1-hexanoyl-3-(4-*p*-tolylethynylphenyl)-thiourea (**APHX**), see Fig. 1, has been successfully prepared and characterized. **APHX** consists of donor-π-donor (D-π-D) system with hybrid functional substructures including conjugated double and triple bonds together with reactive carbonyl (C═O) and thiocarbonyl (C═S) groups, which supposed to play significant role to afford an ideal interaction with VOCs. Thus, the compound has been further used as active material in the preparation of thin-film onto glass substrate entrapped with PVC for VOCs molecular sensor. Moreover, spectroscopic studies of the fluctuations in electronic transition profiles of the material in the form of thin-film exposed to benzene have been performed. **APHX** has shown to be a good candidate for the detection of benzene in gas phase, with high sensitivity and fast response. To support the findings, the stabilisation energy and interaction geometry between **APHX** and benzene have been modelled by using quantum chemical calculations.

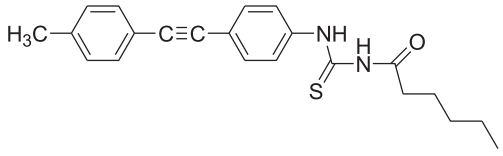

Fig. 1. Molecular structure of **APHX**.

2. Experimental

2.1. Materials

Solvents, chemicals and reagents used in this study namely acetone, acetonitrile, chloroform, dichloromethane, methanol, triethylamine, 4-iodoaniline, ethynyltoluene, palladium(II) chloride, copper(I) iodide, ammonium thiocyanate, and hexanoyl chloride were commercially purchased from local suppliers as analytical reagents such as Fisher Scientific, Merck, HmbG® Chemicals and R&M Chemicals. They were used as received without any further purification carried out. Besides, all reactions involved were executed under an ambient atmosphere without precaution steps to omit humidity during experimental work-up.

2.2. Characterisation and instrumentation

Fourier Transform Infrared (FT-IR) analysis was analysed via Perkin Elmer 100 FT-IR spectroscopy using potassium bromide (KBr) pellets within spectral range 4000-450 cm^{-1}. For structural analysis, ^{1}H and ^{13}C Nuclear Magnetic Resonance (NMR) spectra were recorded in $CDCl_3$ using Bruker Avance III 400 Spectrometer in the presence of trimethylsilane (TMS) as internal standard in the range δ_H 0–15 ppm and δ_C 0–200 ppm respectively. In addition, for electronic transition analysis, the compound was characterised via UV–visible analysis using Shimadzu UV–Vis in 1 cm^3 cuvette. Meanwhile, for structural elucidation, the crystallographic structure for X-ray analysis was analysed on Bruker SMART APEXII Duo CCD area-detector diffractometers using MoKα radiation (λ = 0.71073 Å). Afterwards, thermogravimetric analysis was carried out using Perkin-Elmer TGA analyzer from 30 to 900 °C at a heating rate 10 °C/min under nitrogen flow consistently. Lastly, density functional theory (DFT) was calculated for final molecule using Gaussian 09 at the theoretical level of DFT B3LYP/6-31G (d,p) to calculate HOMO-LUMO behaviours as well as to evaluate the stabilisation energy (kJ/mol) and interaction distance between synthesised compound and targeted analyte (benzene).

2.3. Sonogashira cross-coupling reaction: synthesis of 4[4-aminophenyl] ethynyltoluene (*APE*)

Reaction work-up details with respect to the synthesis of precursor (**APE**) followed as stated in the previous literature [24]. Into a 100 ml round bottom flask was charged 4-iodoaniline (3.0 g, 13.7 mmol), ethynyltoluene (3.28 ml, 25 mmol), triethylamine (10 mL), and water as a solvent (30 mL) via $Pd(PPh_3)_2Cl_2$/CuI-catalysed (0.05 mmol%). The flask was put at reflux to 180 °C for 24 h. The reaction was monitored by using thin layer chromatography

(TLC) in solvent system (hexane: methylene chloride: 3:2). Later, the resulting solution was poured into a separation funnel and the organic phase was extracted via liquid-liquid extraction method using methylene chloride (CH_2Cl_2). Sodium sulphate (Na_2SO_4) was added into the collected organic phase to get rid of water molecules and evaporated under vacuum leaving the crude product. The crude product was then purified via column chromatography (hexane: methylene chloride: 7:3). Evaporation of solvents under reduced pressure afforded the product of **APE** (0.45 g, 95% yield) as brown solid. $C_{15}H_{13}N$ requires: C, 86.95; H, 6.28; N, 6.76. Found: C, 87.59; H, 6.41; N, 6.77%. ^{1}H NMR ($CDCl_3$), 400.11 MHz): δ 2.34 (s, 3H, CH_3); 3.77 (s, br, 2H, NH_2); 6.62 (pseudo-d, $^3J_{HH}$ = 9 Hz, 2H, C_6H_4); 7.13 (pseudo-d, $^3J_{HH}$ = 8 Hz, 2H, C_6H_4); 7.31 (pseudo-d, $^3J_{HH}$ = 9 Hz, 2H, C_6H_4); 7.37 (pseudo-d, $^3J_{HH}$ = 8 Hz, 2H, C_6H_4). ^{13}C NMR ($CDCl_3$, 100.61 MHz): δ 21.5 (CH_3); 87.4, 89.3 (C≡C); 112.8, 116.7, 122.8, 129.0, 133.2, 134.9, 137.7, 146.5 (Ar).

2.4. Synthesis of 1-hexanoyl-3-(4-p-tolylethynyl-phenyl)-thiourea (*APHX*)

The general synthetic pathway to synthesis **APHX** is as shown in Scheme 1. Hexanoyl chloride (0.325 g, 2.42 mmol) in 10 ml acetone was put to react along with ammonium thiocyanate solution (0.184 g, 2.42 mmol) in 10 ml of acetone. The reaction was put at reflux for *ca.* 4 h to give clear solution and white precipitate of ammonium chloride. The dissolved **APE** in 10 ml acetone was later charged into the reaction mixture and refluxed for another *ca.* 4 h. Once reaction adjudged completion by using thin layer chromatography (TLC) in solvent system (hexane: methylene chloride: 3:2), the mixture was cooled to ambient temperature and filtered into beaker containing ice cubes and yellow precipitate was obtained. It was recrystallized from acetonitrile to afford pale yellowish crystalline solids of **APHX** (0.38 g, 70% yield). $C_{22}H_{24}N_2OS$ requires: C, 72.51; H, 6.59; N, 7.62; S, 8.42. Found: C, 72.06; H, 6.65; N, 7.62; S, 8.42%. ^{1}H NMR ($CDCl_3$), 400.11 MHz): δ 0.93 (s, 3H, CH_3); 1.36 (m, 4H, CH_2); 1.70 (m, 2H, CH_2); 2.38 (t, 5H, CH_2CH_3); 7.17 (pseudo-d, $^3J_{HH}$ = 8 Hz, 2H, C_6H_4); 7.41 (pseudo-d, $^3J_{HH}$ = 8 Hz, 2H, C_6H_4); 7.55 (pseudo-d, $^3J_{HH}$ = 8 Hz, 2H, C_6H_4); 7.70 (pseudo-d, $^3J_{HH}$ = 8 Hz, 2H, C_6H_4); 8.75 (s, 1H, NH); 12.50 (s, 1H, NH). ^{13}C NMR ($CDCl_3$, 100.61 MHz): δ 13.90 (Ar–CH_3); 21.5 (CH_2CH_3); 88.2, 90.2 (C≡C); 120.0, 121.8, 123.4, 125.1, 128.3, 129.8, 131.0, 133.1 (C–Ar); 174.2 (C=O); 177.7 (C=S).

2.5. Fabrication of *APHX* on glass substrate

APHX was fabricated on the glass surface via drop-casting method. The solution was prepared in 5% w/w ratio of **APHX** which included polyvinyl chloride (PVC) and tributylphosphate as plasticizer in 5 ml tetrahydrofuran (THF) with continuous stirring for *ca.* 3 h to achieve complete homogeneity. The obtained films were kept in a dried and closed desiccator to avoid any undesired interaction with any gas in atmosphere. Properties of absorption spectra of the thin film before and after exposure were compared to determine the response towards selected VOC (benzene).

2.6. Investigation of sensing performance

The response of **APHX** thin film as optical gas sensor in four different time intervals was investigated by **APHX** thin film was exposed to vapor of benzene in a close vessel and measured *in-situ* by using UV–visible spectrophotometer (Shimadzu 1601 series). The obtained absorbance values were used to calculate the response of **APHX** thin film towards benzene using Equation (1), where A(vap) represents the absorbance of thin film after exposed to vapours of benzene, A(ref) represents the absorbance of **APHX** thin film before exposed to benzene, and S represents the percentage response of **APHX** with benzene.

$$S = \frac{|A(vap) - A(ref)|}{A(ref)} \times 100 \quad (1)$$

2.7. Structure refinement and X-ray data collection of *APHX*

X-ray analysis of a suitable yellowish needle-shape single crystal (0.62 mm × 0.16 mm x 0.13 mm) was performed on Bruker SMART APEXII Duo CCD area-detector diffractometers using MoKα radiation (λ = 0.71073 Å). Data collection was performed using the APEX2 software [30]. For the cell refinement and data reduction process, the SAINT software [31] was used. The molecular structure of **APHX** was solved by direct method using the program SHELXTL [31] and refined by full-matrix least squares technique on F^2 using anisotropic displacement parameters by SHELXTL [31]. The empirical absorption correction was applied to the final crystal data using the SADABS software [30]. All geometrical calculations were

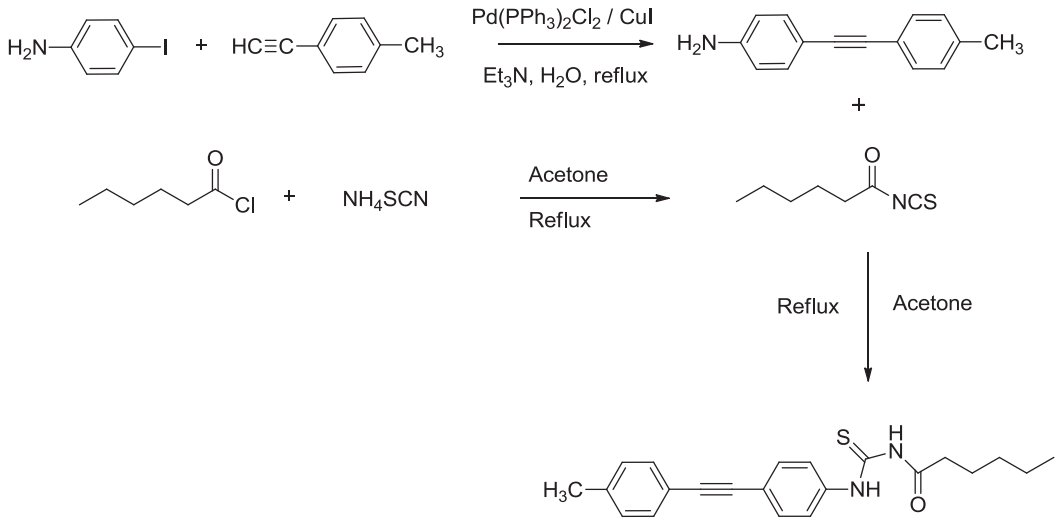

Scheme 1. General synthetic work-up to obtain acetylide-thiourea derivative (**APHX**).

carried out using the program PLATON [32] and the 3-dimensional molecular graphics were drawn using SHELXTL [31] and Mercury program [33]. The non-hydrogen atoms were refined anisotropically. In this compound, all the hydrogen atoms were positioned geometrically with C–H bond distance of 0.93 Å and refined using riding model where the isotropic displacement parameters set to 1.2(C) and 1.5(C_{methyl}) times the equivalent isotropic U values of the parent carbon atoms. In addition, a rotation model (AFIX 137) was applied to the methyl groups. The N-bound hydrogen atoms was located in a difference Fourier map and refined freely [refined N–H distance = 0.758 (19) – 0.81 (2) Å]. In the final refinement, the most disagreeable reflection was omitted (0 0 1). The relevant refinement parameters of **APHX** are listed in Table 1. Crystallographic information file has been deposited in Cambridge Structure database (CCDC 1500205).

3. Results and discussion

3.1. Crystallographic structural analysis of *APHX*

A yellow needle-shape crystal of 1-hexanoyl-3-(4-*p*-tolylethynyl-phenyl)-thiourea (**APHX**) was crystallised from slow evaporation process in acetonitrile at room temperature. The molecular structure of 1-hexanoyl-3-(4-*p*-tolylethynyl-phenyl)-thiourea (**APHX**) was determined by the result of a single crystal X-ray structure determination as triclinic crystal system in P-1 space group; unit cell, a = 9.5729(4)Å, b = 11.5325(5)Å, c = 18.9624(8)Å, α = 100.903(2)°, β = 96.351(2)°, γ = 90.064(2)° and Z = 4. The molecular structure of **APHX** is shown in Fig. 2. The asymmetric unit of **APHX** contains two crystallographically independent molecules, A and B. The molecules (A and B) adopt *trans-cis* configurations with respect to the position of the hexanoyl (O1/C17–C22) and 1-methyl-4-(phenylethynyl)benzene (C1–C15) moieties relatively to the thiocarbonyl sulphur (S1) atom across the C16–N2 and C16–N1 bonds, respectively. Fig. 2 (a) shows both molecules (A and B) are stabilized by the intramolecular N–H···O and C–H···S hydrogen bonds (Supplementary Information 1) which leads to the formation of two six-membered closed loop with graph set notations, S(6). This pseudo ring motif has been recognized as a key factor for the molecular conformation since it forms the barriers to single bond rotating and further favouring a nearly planar arrangement [34]. In molecule A, the maximum deviation from local planarity of the carbonyl thiourea [–C(O)NHC(S)NH–] group is 0.0158(16)Å at atom N2A while the corresponding maximum deviation value is 0.0189(19)Å at atom C17B in molecule B. This nearly planar carbonyl thiourea moiety forms dihedral angles of 82.64(16)° and 27.12(7)° with the alkyl chain (C18A-C22A) and 1-methyl-4-(phenylethynyl)benzene moiety (C1A-C15A) in molecule A. Meanwhile, in molecule B the nearly planar carbonyl thiourea plane makes dihedral angles of 81.61(16)° and 28.98(16)° with C18B–C22B and C1B–C15B, respectively. Both molecules are found to be slight twisted at the C19–C18–C17–O1 and C14–C13–N1–C16 torsion angles of 18.3(3)° and 29.9(3)° in molecules A and −18.1(3)° and 28.9(3)° in molecule B. The twisted structure of the molecules is shown as in Fig. 2 (b). Additionally, the dihedral angles between the benzene rings (C2–C7 and C10–C15) are 0.65(10)° and 1.23(9)° in molecule A and B, respectively.

Table 2 lists the selected bond lengths and angles where all bond lengths and angles are found to be very close with the previously reported structures of carbonyl thiourea [35–37]. The molecular structure of **APHX** subsists as thione form with typical thiourea moieties of C=O and C=S double bonds as well as the shortened of C–N bond lengths. In molecules A and B, the carbonyl (C17–O1) bond lengths are found to be 1.213(2)Å whereas the thiocarbonyl (C16–S1) bond lengths are 1.6657(18)Å in A and 1.6635(18)Å in B, showing the typical double bond characters. The C–N bond lengths (N1–C16, C16–N2 and N2–C17) of the investigated thiourea derivative of **APHX** are all shorter than the average single C–N bond length (1.48 Å) and slightly longer than the double C–N bond length (1.32 Å) where the values are 1.331(2)Å, 1.387(2)Å and 1.375(2)Å in molecule A, respectively. The corresponding bond length values in molecule B are 1.333(2)Å, 1.388 (2)Å and 1.371(2)Å. The varying degrees of in these C–N bond lengths indicate the partial electron delocalization within the N1–C16–N2–C17 fragment. In both molecules, the N1–C16 bond lengths is longer than N1–C16 bond lengths which is probably due to the electron withdrawing effect of the carbonyl group [38]. Furthermore, the bond angles values of C13–N1–C16 [molecule A = 130.11 (16)° and molecule B = 130.06 (16)°] and C16–N2–C17 [molecule A = 129.62 (17)° and molecule B = 129.65 (17)°] show the sp^2 hybridization on atoms N1 and N2.

In the crystal packing of **APHX** (Fig. 3), intermolecular C18B–H18C···S1A, N2B–H2NB···S1A and N2A–H2NA···S1B hydrogen bonds (Supporting Information 1) link the molecules into a centro-symmetric dimers [39] forming R22(8) and R21(6) graph-set motifs [40]. These dimers are stacked along the *a*-axis. The crystal structure is consolidated by the intermolecular C–H···π interactions (see Supporting Information 1) and further link the dimers into an infinite one-dimensional column parallel to the *a*-axis.

Table 1
Crystal data and structure refinement.

Refinement parameters	
CCDC deposition numbers	1500205
Molecular formula	$C_{22}H_{24}N_2OS$
Molecular weight	364.49
Crystal system	Triclinic
Space group	*P*-1
a/Å	9.5803 (9)
b/Å	11.5178 (10)
c/Å	18.9403 (17)
α/°	100.903 (2)
β/°	96.394 (2)
γ/°	90.107 (2)
V/Å^3	2038.9 (3)
Z	4
D_{calc} (g cm^{-3})	1.187
Crystal Dimensions (mm)	0.62 × 0.16 × 0.13
μ/mm^{-1}	0.17
Radiation λ (Å)	0.71073
F(000)	776
T_{min}/T_{max}	0.902/0.978
Reflections measured	46996
Ranges/indices (*h*, *k*, *l*)	*h* = −12 → 12 *k* = −14 → 14 *l* = −24 → 24
θ limit (°)	1.8–27.6
Unique reflections	9424
Observed reflections ($I > 2\sigma(I)$)	5430
Parameters	489
R_1[a], wR_2 [b]$[I \geq 2\sigma(I)]$	0.049/0.152
Goodness of fit [c] on F^2	1.02
R_{int}	0.044
Largest diff. peak and hole, e/Å^{-3}	0.22 and −0.20

[a-c] represent unit cell parameters in x-ray crystallography.

3.2. Spectroscopic studies

FT-IR analysis of **APHX** showed five characteristic bands for the acyl-thiourea and acetylide groups, namely; ν(N–H), ν(C≡C), ν(C–H), ν(C=O), and ν(C=S). The band occurring at 3185 cm^{-1} can be consigned to the vibration of functional group (N–H) in the secondary thioamide group. The value shifted to the low

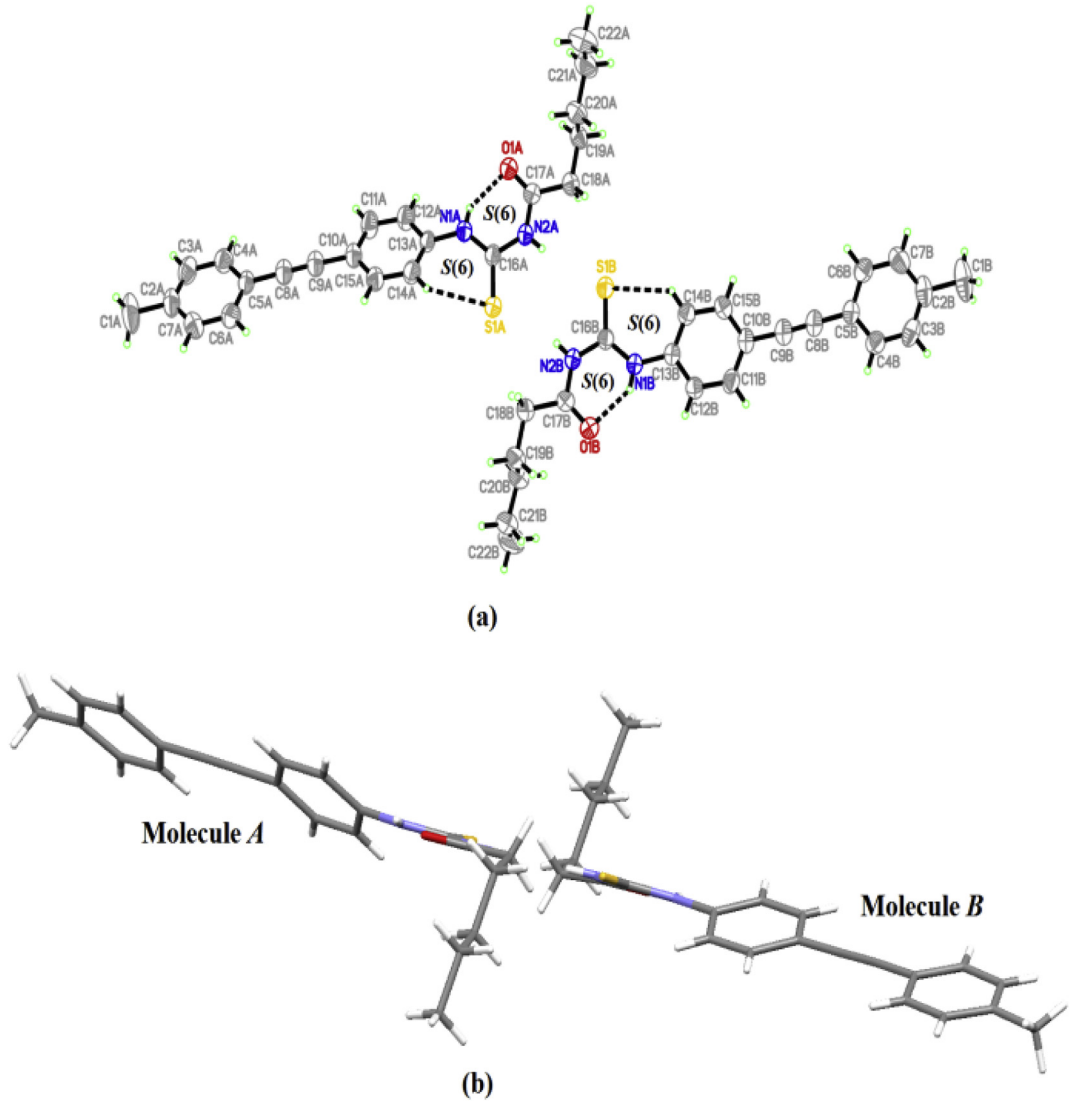

Fig. 2. (a) **APHX** molecular structure diagram with 50% ellipsoids probability of the compound embedded with atomic numbering scheme and dashed lines represent the intramolecular hydrogen bonds (b) The twisted view of the molecules A and B.

wavelength indicated the behaviour of intramolecular hydrogen bonding [41,42]. Strong absorption band of the (C═O) stretching vibration is located at 1653 cm^{-1} [43,44] a slightly lower values from ordinary amide carbonyl absorption (1670 cm^{-1}), probably due to the effects of intramolecular hydrogen bonding with N–H and electron donating presence (alkyl group) in which weakened the carbonyl bond. Additionally, persistence of a band at around 2935 cm^{-1} was due to the presence of (C–H) stretching vibration of alkyl chain. The band expected from the acetylide group (C≡C) occurred at 2215 cm^{-1} in good agreement with previous literature for related kind [45]. The thiourea group shows the occurrence of a band at 743 cm^{-1} allocated to the ν(C═S) with partially double bond character and low nucleophilic character of sulfur atom [46,47].

3.3. *UV–visible studies and frontier molecular orbitals of **APHX***

The absorption spectrum of **APHX** was carried out in acetonitrile which comprises two major bands as shown in Fig. 4. The strongest band occurred in the region of 275 nm (ε = 50,000 L mol^{-1} cm^{-1}) which was assigned predominantly due to π–π* transition which was expected to arise from phenyl rings and acetylide (C≡C) moieties. In fact, the π–π* transition shifted to longer wavelength due to the effect of π-conjugation of acetylide derivatives. Particularly, the second band appeared in the region of 330 nm (ε = 30,000 L mol^{-1} cm^{-1}), was assigned also as π–π* transition which was consigned for the presence of amine (N–H), carbonyl (C═O) and thione (C═S) moieties [48]. Consequently, the energy band gap (E_g) of **APHX** was calculated from the UV–vis absorption maximum (λ_{max}) of the compound within range 200–500 nm. From UV–vis data, the E_g for **APHX** is 3.75 eV in which **APHX** is classified as semiconductor material.

The frontier molecular orbital analysis is a vital part in the development of molecular electronic properties. The TD-DFT calculated electronic absorption spectrum and the maximum absorption wavelength were revealed to have good agreement with the electronic transition from HUMO to LUMO. In fact, the energy gap (E_g) between HOMO and LUMO is a crucial factor in defining molecular electrical transport properties. In this present analysis, the HOMO and LUMO were computed at TD-SCF B3LYP/6-31G (d,p) theoretical and its respective plot of the frontier molecular orbital are as illustrated in Fig. 5. Results obtained revealed that HOMO is

Table 2
Selected bond lengths (Å) and bond angles (°) for **APHX**.

	Molecule *A*	Molecule *B*
Bond Lengths (Å)		
C17–O1	1.213 (2)	1.213 (2)
C16–S1	1.6657(18)	1.6635 (18)
C13–N1	1.419 (2)	1.419 (2)
N1–C16	1.331 (2)	1.333 (2)
C16–N2	1.387 (2)	1.388 (2)
N2–C17	1.375 (2)	1.371 (2)
C8–C9	1.198 (2)	1.194 (3)
Bond Angles (°)		
O1–C17–N2	122.38 (17)	122.57 (17)
C18–C17–N2	114.36 (16)	114.02 (16)
C17–N2–C16	129.62 (17)	129.65 (17)
N2–C16–S1	118.23 (13)	118.36 (13)
N2–C16–N1	114.96 (16)	114.61 (16)
S1–C16–N1	126.81 (14)	127.03 (13)
C16–N1–C13	130.11 (16)	130.06 (16)
Torsion Angles (°)		
C19 –C18–C17–O1	18.3 (3)	–18.1 (3)
C19–C18–C17–N2	–163.24 (17)	163.23 (17)
C18–C17–N2–C16	–175.31 (18)	173.98 (18)
O1–C17–N2–C16	3.1 (3)	–4.7 (3)
C17–N2–C16–S1	177.64 (16)	–177.96 (16)
C17–N2–C16–N1	–1.7 (3)	2.9 (3)
N2–C16–N1–C13	179.87 (17)	–177.29 (17)
S1–C16–N1–C13	0.6 (3)	3.7 (3)
C12–C13–N1–C16	–154.5 (2)	–154.44 (19)
C14–C13–N1–C16	29.9 (3)	28.9 (3)

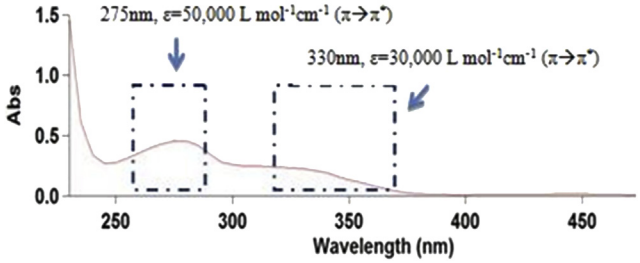

Fig. 4. The UV–vis absorption spectrum of **APHX.**

between HOMO and LUMO was nominated by involving π-π* bonding system localized around phenyl moiety and an orbital of p-type generally localized over sulfur atom [39,49,50]. Indeed, the energy gap obtained is 3.8 eV, mostly responsible for the charge and electron transition that occurred within the molecule [51] in qualitative good agreement with the experimental electronic spectrum.

3.4. Thermal behaviour analysis of ***APHX***

Fig. 6 shows thermogravimetric analysis for **APHX**. The thermal stability of sensory material is an important part to be determined for any gas sensing application involving high temperature. **APHX**

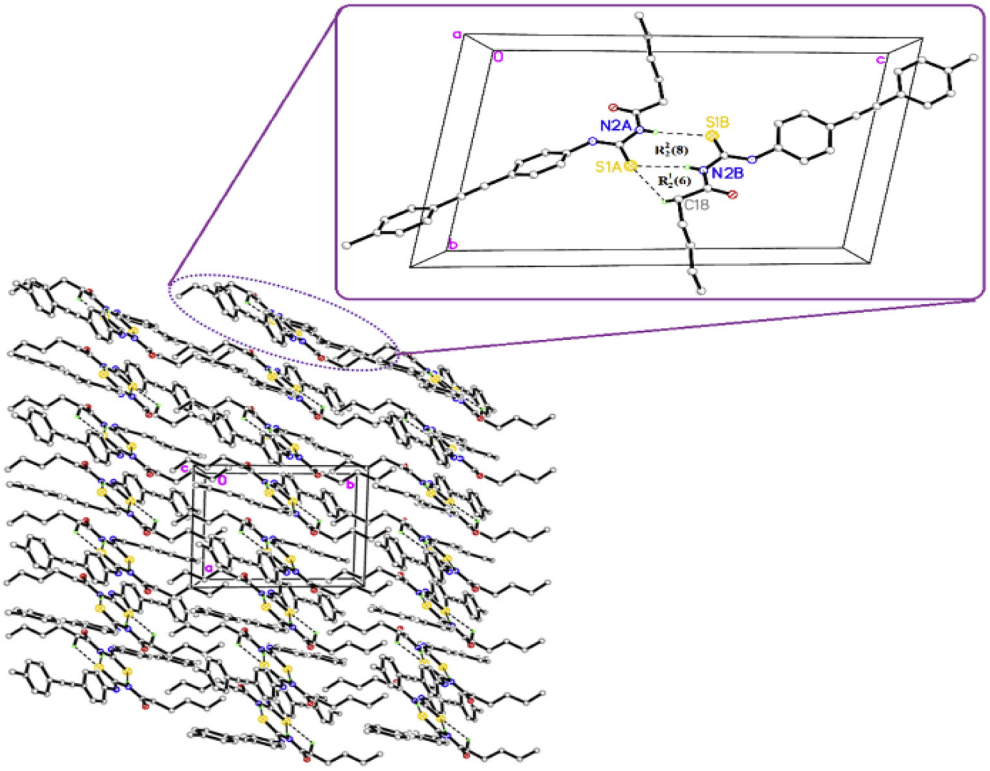

Fig. 3. Packing diagram view of **APHX**. H atoms are omitted for clarity.

characterized as an extended π system delocalized throughout the phenyl group, the –C≡C– triple bond acting as a bridge, including the thioacetamide group [π(C═O) and the sulphur lone pair]. The LUMO also comprises antibonding system with local π symmetry extended over the aromatic rings including the acyl thiourea π*(C═O) and π*(C═S) antibonding orbitals. Thus, the interaction

thermal analysis was examined via TGA-DTG at heating rate of 10 °C/min under nitrogen atmosphere temperature range from 30 to 900 °C. The molecule is stable up to ca. 192 °C and the first decomposition stage occurred at 195 °C (onset) and ended at 280 °C (offset), while the next stage started to degrade at 372 °C (onset) and ended at 458 °C (offset) with the maximum degradation of

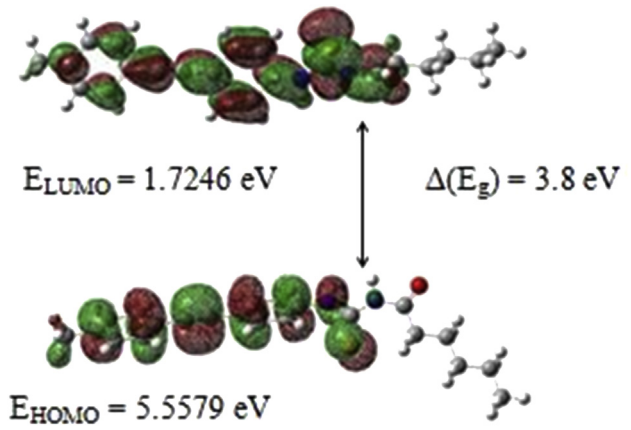

Fig. 5. Molecular orbitals involved during electronic transition between HOMO-LUMO of **APHX.**

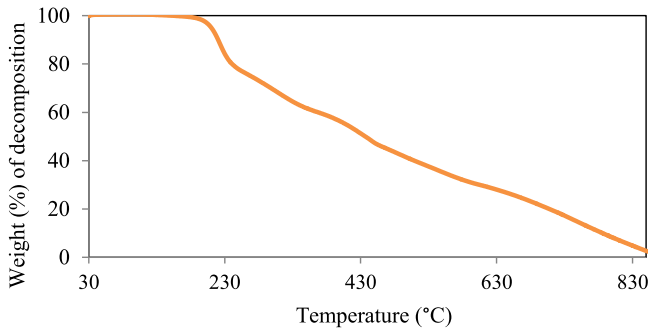

Fig. 6. Thermogravimetric thermogram analysis of **APHX.**

201 °C and 467 °C respectively. Therefore, **APHX** exhibited high stability due to their large range of decomposition between their onset and offset temperature from every stage of degradation. Indeed, the presence of conjugated molecule with π-stacking between aromatic moieties, C═O and C═S moieties gave high thermal stability of the synthesised compound which provided initial indication for this molecule can be used at high temperature.

3.5. Sensing studies of APHX towards benzene via UV–visible spectroscopy analysis

Sensing studies of **APHX** in the form of thin-film acting as sensor was investigated towards pure benzene. The absorption spectrum of the optical VOC sensor with various time of exposure towards **APHX** thin-film was inspected in advance to define the sensitivity response of the film substrate for the detection vapour of benzene. Results obtained from absorption spectrum indicated the important alterations had occurred in the electronic transition of **APHX** thin-film before and after exposure towards benzene in four different time intervals. Upon interaction with benzene, the band at 330 nm showed to be the most affected absorption in the electronic spectrum, accounting for a change in the HOMO/LUMO levels of **APHX**. Results indicated, upon exposure of **APHX** towards benzene to an increasing time intervals, the maximal absorbance of the film-substrate decreased to a lower absorbance, indicating that an interaction of **APHX** film substrate with benzene has occurred. **APHX** molecule containing electron donating substitution (alkyl group) exhibited high response towards benzene with elongation of time intervals, with 10% for 5 s exposure, 25%, 35%, and 48% for 15 min, 20 min, and 1 h exposure time respectively. The VOC sensor response of **APHX** increased without sign of saturation due to the effect of electron donating substitution consists of sufficient electron density which enables the interaction with the π-molecular orbital of benzene. Fig. 7 shows the sensor response bar chart of the film substrate of **APHX** to benzene from 5 s to 1 h of time exposure. This result seems to be in same arguments with those findings reported in previous occasions [24,52].

3.6. Theoretical calculations: prediction of sensor-analyte molecular interaction

In order to determine possible interaction sites and geometries, different pairs of **APHX**:benzene dimers was subject of optimization procedure using quantum chemical calculations at the B3LYP/6-31G(d,p) level of approximation. Fig. 8 shows the predicted molecular structure of the more stable configuration obtained for a pair of **APHX** and benzene molecule. The benzene molecule interacts mainly with the acyl-thiourea group of **APHX**. To understand the nature of the interaction between **APHX** and benzene, the Mulliken charges values on the selected atoms were measured (as in Fig. 8) as well as the interaction distance for the optimized structure are as listed in Table 3.

The charge on the oxygen atom of (C═O amide) lower than that of the hydrogen on nitrogen atom of (N–H) in thiourea moiety which was observed to be in the range −0.53, compared to hydrogen atom which about 0.28 (N–H(1)) and 0.33 (N–H(2)). The interactions which were formed between **APHX** and benzene are possible to interact at the oxygen atom of (C═O amide) forming H-bonding due to the high negative charge value on oxygen atom, and less steric hindrance compared to other possible sites.

In addition, the total electronic energies of **APHX** and the stabilisation energies of the individual **APHX** and benzene molecule are calculated to investigate the stabilization interaction at the possible sites. Results revealed that **APHX** was sensitive material for detection of benzene with the stabilisation energy value of −23.69 kJ/mol, demonstrate a strong coulombic interaction as well as indicating H-bonding interaction occurred, which has caused by fluctuation of electron density between the interacting atoms.

4. Conclusions

A new acetylide-thiourea derivative 1-hexanoyl-3-(4-*p*-tolylethynyl-phenyl)-thiourea (**APHX)** has been synthesised and characterised as active compound for using as thin-film membrane supported with PVC matrix for the detection of VOC analyte, namely benzene. The molecular structure of the crystal is characterized by a nearly planar arrangement extended through the (4-*p*-

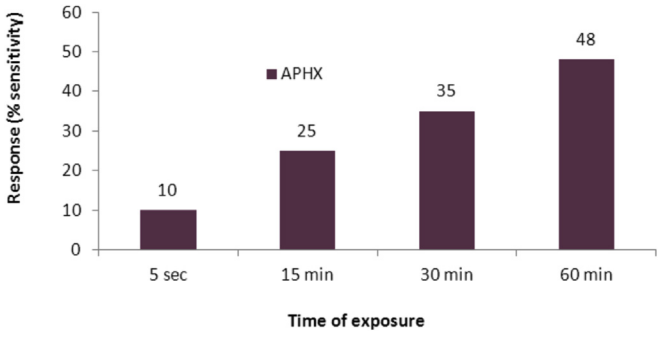

Fig. 7. Changes in the absorbance value of the 330 nm band of **APHX** with increasing time of exposure towards benzene.

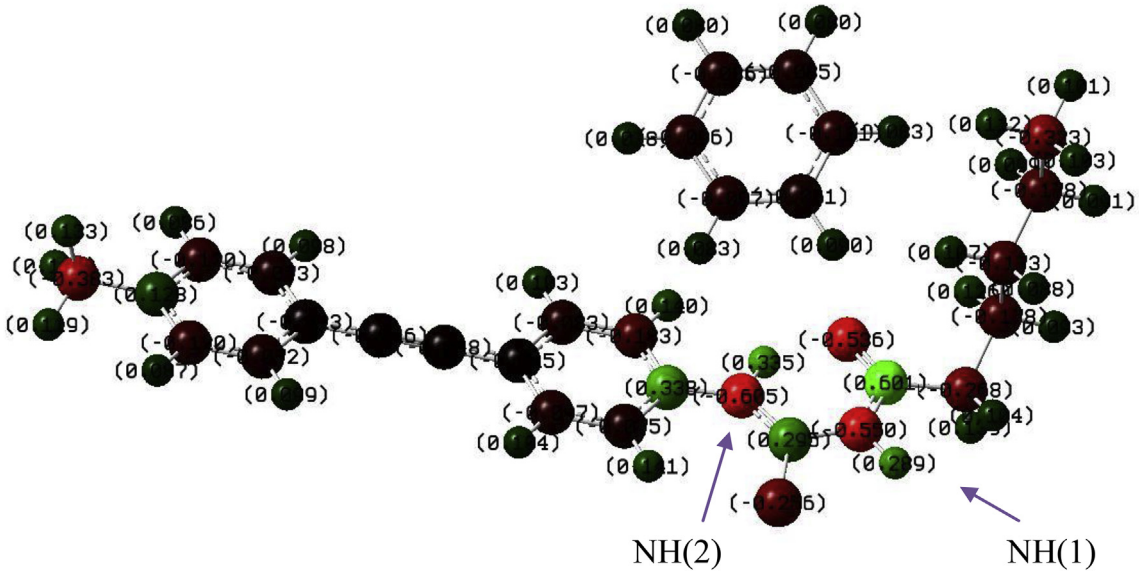

Fig. 8. The predicted possible interaction between **APHX** and benzene.

Table 3
The interaction distance between benzene and C═O and NH.

Molecule	Calculated distance between benzene and C═O; NH (Á)		
	O (C═O)	H (NH(1))	H (NH(2))
APHX	H–O 2.7	C–H 2.7	C–H 2.9

tolylethynyl-phenyl)-thiourea group, the C═O double bond of the hexanoyl substituent favours the formation of a N–H···O═C intramolecular hydrogen bond. The UV–Vis spectrum of **APHX** is consistent with a highly delocalized electronic π-system. The sensitivity of the film substrate to vapours of benzene at room temperature was investigated using the difference features in electronic transition spectra upon interaction with benzene. **APHX** exhibited good response with almost 48% response in 1 h of time exposure operated at room temperature. In fact, theoretical calculation proved that **APHX** showed ideal interaction energies (−23.69 kJ/mol) for sensing benzene analyte. Hence, the approach of molecular system featuring acetylide-thiourea (**APHX**) revealed promising ability and potential to act as active layer for detection of benzene.

Acknowledgements

The authors would like to thank the Ministry of Higher Education Malaysia (MOHE) for the research grant ERGS 55102, SLAB/SLAI and Universiti Malaysia Perlis (UniMAP) for postgraduate student's scholarship, and the School of Fundamental Science, Universiti Malaysia Terengganu for facilities and research aids. MFE is a member of the Carrera del Investigador of CONICET (República Argentina). The Argentinean author thanks to the Consejo Nacional de Investigaciones Científicas y Técnicas (CONICET), the ANPCYT (PICT-2130) and the Facultad de Ciencias Exactas, Universidad Nacional de La Plata for financial support.

Appendix A. Supplementary data

Supplementary data related to this article can be found at http://dx.doi.org/10.1016/j.molstruc.2017.03.065.

References

[1] B. Yuliarto, Y. Kumai, S. Inagaki, H. Zhou, Enhanced benzene selectivity of mesoporous silica SPV sensors by incorporating phenylene groups in the silica framework, Sens. Actuat. B Chem. 138 (2) (2009) 417–421.
[2] H. Wen, L. Yuan, C. Wei, Y. Zhao, Y. Qian, P. Ma, D. Shumao, Y. Xu, X. Wang, Effects of combined exposure to formaldehyde and benzene on immune cells in the blood and spleen in balb/c mice, Environ. Toxicol. Phar 45 (2016) 265.
[3] M. Mascelloni, J.M. Delgado-Saborit, N.J. Hodges, R.M. Harrison, Study of gaseous benzene effects upon A549 lung epithelial cells using a novel exposure system, Toxicol. Lett. 237 (1) (2015) 38–45.
[4] N.A. Philbrook, L.M. Winn, Investigating the effects of in utero benzene exposure on epigenetic modifications in maternal and fetal CD-1 mice, Toxicol. Appl. Phar 289 (1) (2015) 12–19.
[5] Z. Zhang, X. Wang, Y. Zhang, S. Lü, Z. Huang, X. Huang, Y. Wang, Ambient air benzene at background sites in China's most developed coastal regions: exposure levels, source implications and health risks, Sci. Total. Environ. 511 (2015) 792–800.
[6] V.S. Vaishnav, S.G. Patel, J.N. Panchal, Development of ITO thin film sensor for detection of benzene, Sens. Actuat. B Chem. 206 (2015) 381–388.
[7] C. Murugan, E. Subramanian, D.P. Padiyan, p–n Heterojunction formation in polyaniline–SnO_2 organic–inorganic hybrid composite materials leading to enhancement in sensor functionality toward benzene and toluene vapors at room temperature, Synth. Met. 192 (2014) 106–112.
[8] Y. Zhao, W. Lu, H. Wang, Volatile trace compounds released from municipal solid waste at the transfer stage: evaluation of environmental impacts and odour pollution, J. Hazard. Mater 300 (2015) 695–701.
[9] Y. Liu, J. Chen, W. Li, D. Shen, Y. Zhao, M. Pal, Y. Haijun, T. Bo, D. Zhao, Carbon functionalized mesoporous silica-based gas sensors for indoor volatile organic compounds, J. Colloid. Interf. Sci. 477 (2016) 54–63.
[10] S. Chatterjee, M. Castro, J.F. Feller, Tailoring selectivity of sprayed carbon nanotube sensors (CNT) towards volatile organic compounds (VOC) with surfactants, Sens. Actuat. B Chem. 220 (2015) 840–849.
[11] P. Kumar, A. Deep, K.H. Kim, R.J. Brown, Coordination polymers: opportunities and challenges for monitoring volatile organic compound, Prog. Polym. Sci. 45 (2015) 102–118.
[12] A. Daneshkhah, S. Shrestha, M. Agarwal, K. Varahramyan, Poly (vinylidene fluoride-hexafluoropropylene) composite sensors for volatile organic compounds detection in breath, Sens. Actuat. B Chem. 221 (2015) 635–643.
[13] Y. Wei, L. Luo, Y. Ding, X. Si, Y. Ning, Highly sensitive determination of methotrexate at poly (l-lysine) modified electrode in the presence of sodium dodecyl benzene sulfonate, Bioelectrochemistry 98 (2014) 70–75.
[14] M. Farbod, M.H. Joula, M. Vaezi, Promoting effect of adding carbon nanotubes on sensing characteristics of ZnO hollow sphere-based gas sensors to detect volatile organic compounds, Mater. Chem. Phys. 176 (2016) 12–23.
[15] H.M. Aliha, A.A. Khodadadi, Y. Mortazavi, The sensing behaviour of metal oxides (ZnO, CuO and Sm_2O_3) doped-SnO_2 for detection of low concentrations of chlorinated volatile organic compounds, Sens. Actuat. B Chem. 181 (2013) 637–643.
[16] C. Murugan, E. Subramanian, D.P. Padiyan, Enhanced sensor functionality of in

situ synthesized polyaniline–SnO2 hybrids toward benzene and toluene vapors, Sens. Actuat. B Chem. 205 (2014) 74–81.
[17] A.I. Daud, W.M. Khairul, H. Mohamed Zuki, K. KuBulat, Synthesis and characterization of N-(4-Aminophenylethynylbenzonitrile)-N′-(1-naphthoyl) thiourea as single molecular chemosensor for carbon monoxide sensing, J. Sulfur. Chem. 35 (6) (2014) 691–699.
[18] R. Rahamathullah, W.M. Khairul, K. Ku Bulat, Z.M. Hussin, Influence of curcumin as a natural photosensitizer in the conductive thin film of alkoxy cinnamoyl substituted thiourea, Main. Group Chem. 14 (3) (2015) 185–198.
[19] W.M. Khairul, A.I. Daud, H. Mohamed Zuki, K. Kubulat, Theoretical and spectroscopic studies of N-([4-aminophenyl] ethynyltoluene)-N'-(1-naphthanoyl thiourea (ATT) as carbon monoxide gas chemosensor, Appl. Mech. Mater 719 (2015) 59–62.
[20] A. Saeed, A. Khurshid, J.P. Jasinski, C.G. Pozzi, A.C. Fantoni, M.F. Erben, Competing intramolecular N-H···O-C hydrogen bonds and extended intermolecular network in 1-(4-chlorobenzoyl)-3-(2-methyl-4-oxopentan-2-yl) thiourea analyzed by experimental and theoretical methods, Chem. Phys. 431 (2014) 39–46.
[21] A. Singh, M.K. Bharty, P. Bharati, A. Bharti, S. Singh, N.K. Singh, N.K. Synthesis, Spectral, thermal and structural characterization of a hexanuclear copper(I) cluster and a cobalt(III) complex of 1-ethyl-3-phenyl-thiourea, Polyhedron 85 (2015) 918–925.
[22] D.M. Gil, M.D. Lestard, O. Estévez-Hernández, J. Duque, E. Reguera, Quantum chemical studies on molecular structure, spectroscopic (IR, Raman, UV–Vis), NBO and HOMO–LUMO analysis of 1-benzyl-3-(2-furoyl) thiourea, Spectrochim. Acta.A 145 (2015) 553–562.
[23] W.M. Khairul, M.F. Abu Hasan, A.I. Daud, H. Mohamed Zuki, K. Kubulat, M.A. Kadir, Theoretical and experimental investigation of pyridylthiourea derivatives as ionophores for Cu(II) ion detection, Malays. J. Anal. Sci. 20 (2016) 73–84.
[24] S. Bilal, S. Bibi, S.M. Ahmad, Counterpoise-corrected energies, NBO, HOMO–LUMO and interaction energies of poly (o-aminophenol) for ammonia sensing by DFT methods, Synt. Met. 209 (2015) 143–149.
[25] A.I. Daud, W.M. Khairul, H.M. Zuki, K. Kubulat, Aerobic synthetic approach and characterisation of some acetylide–thiourea derivatives for the detection of carbon monoxide (CO) gas, J. Mol. Struct. 1093 (2015) 172–178.
[26] P. Liu, C. Shu, L. Liu, Q. Huang, Y. Peng, Design and synthesis of thiourea derivatives with sulfur-containing heterocyclic scaffolds as potential tyrosinase inhibitors, Bioorgan. Med. Chem. 24 (8) (2016) 1866–1871.
[27] A. Bielenica, E. Kędzierska, M. Koliński, S. Kmiecik, A. Koliński, F. Fiorino, S. Beatrice, M. Elisa, C. Angela, R. Ilaria, M. Paola, E.K. Anna, S. Aleksandra, P. Massarelli, 5-HT2 receptor affinity, docking studies and pharmacological evaluation of a series of 1,3-disubstituted thiourea derivatives, Eur. J. Med. Chem. 116 (2016) 173–186.
[28] V.B. Bregović, N. Basarić, K. Mlinarić-Majerski, Anion binding with urea and thiourea derivatives, Coord. Chem. Rev. 295 (2015) 80–124.
[29] A. Saeed, U. Flörke, M.F. Erben, A review on the chemistry, coordination, structure and biological properties of 1-(acyl/aroyl)-3-(substituted) thioureas, J. Sulfur. Chem. 35 (2014) 318–355.
[30] Sadabs Bruker, APEX2 and SAINT, Bruker AXS Inc Madison WI, USA, 2009.
[31] G.M. Sheldrick, A short history of SHELX, Acta. Crystallogr. A64 (2008) 112–122.
[32] A.L. Spek, Structure validation in chemical crystallography, Acta. Crystallogr. D65 (2009) 148–155.
[33] C.F. Macrae, P.R. Edington, P. McCabe, E. Pidcock, G.P. Shields, R. Taylor, M. Towler, J. van de Streek, Mercury: visualization and analysis of crystal structures, J. Appl. Cryst. 39 (2006) 453–457.
[34] O. Hritzová, J. Černák, P. Šafař, Z. Frőhlichová, I. Csőregh, Furan derivatives of substituted phenylthiourea: spectral studies, semi-empirical quantum-chemical calculations and X-ray structure analyses, J. Mol. Struct. 743 (2005) 29–48.
[35] W. Yang, W. Zhou, Z. Zhang, Structural and spectroscopic study on N-2-fluorobenzoyl-N′-4-methoxyphenylthiourea, J. Mol. Struct. 828 (2007) 46–53.
[36] J. Haribabu, G.R. Subhashree, S. Saranya, K. Gomathi, R. Karvembu, D. Gayathri, Synthesis, crystal structure, and in vitro and in silico molecular docking of novel acyl thiourea derivatives, J. Mol. Struct. 1094 (2015) 281–291.
[37] M. Atiş, F. Karipcin, B. Sariboğa, M. Taş, H. Çelik, Structural, antimicrobial and computational characterization of 1-benzoyl-3-(5-chloro-2-hydroxyphenyl) thiourea, Spectrochim. Acta. A. 98 (2012) 290–301.
[38] Z. Weiqun, L. Baolong, C. Yang, Z. Yong, L. Lude, Y. Xujie, The structure and conformation analysis of N-2-fluorobenzoyl-N′-2-methoxyphenylthiourea, J. Mol. Struct. THEOCHEM 715 (2005) 117–124.
[39] L. Dos Santos, L.A. Lima, V. Cechinel-Filho, R. Corrêa, B. De Campos, R.J. Nunes, Synthesis of new 1-phenyl-3-{4-[(2E)-3-phenylprop-2-enoyl]phenyl}-thiourea and urea derivatives with anti-nociceptive activity, Bioorgan. Med. Chem. 16 (18) (2008) 8526–8534.
[40] J. Bernstein, R.E. Davis, L. Shimoni, N.L. Chang, Patterns in hydrogen bonding: functionality and graph set analysis in crystals, Angew. Chem. Int. Ed. Engl. 34 (1995) 1555–1573.
[41] A. Bielenica, J. Stefańska, K. Stępień, A. Napiórkowska, E. Augustynowicz-Kopeć, G. Sanna, M. Silvia, B. Stefano, G. Gabriele, W. Malgorzata, Struga, M, Synthesis, cytotoxicity and antimicrobial activity of thiourea derivatives incorporating 3-(trifluoromethyl) phenyl moiety, Eur. J. Med. Chem. 101 (2015) 11–125.
[42] S.A. Khan, N. Singh, K. Saleem, Synthesis, characterization and in vitro antibacterial activity of thiourea and urea derivatives of steroids, Eur. J. Med. Chem. 43 (10) (2008) 2272–2277.
[43] Z. Ngaini, M.A. Mohd Arif, H. Hussain, E.S. Mei, D. Tang, D.H.A. Kamaluddin, Synthesis and antibacterial activity of acetoxybenzoyl thioureas with aryl and amino acid side chains, Phosphorus. Sulfur 87 (1) (2012) 1–7.
[44] A. Saeed, M.F. Erben, N. Abbas, U. Flörke, Synthesis, crystal X-ray diffraction structure, vibrational properties and quantum chemical calculations on 1-(4-(4 Fluorobenzamido)phenyl)-3-(4-fluorobenzoyl)thiourea, J. Mol. Struct. 984 (1) (2010) 240–245.
[45] M.E.D. Lestard, D.M. Gil, O. Estévez-Hernández, M.F. Erben, J. Duque, Structural, vibrational and electronic characterization of 1-benzyl-3-furoyl-1-phenylthiourea: an experimental and theoretical study, New. J. Chem. 39 (9) (2015) 7459–7471.
[46] F.A. Saad, Synthesis, spectral, electrochemical and X-ray single crystal studies on Ni(II) and Co(II) complexes derived from 1-benzoyl-3-(4-methylpyridin-2-yl) thiourea, Spectrochim. Acta A 128 (2014) 386–392.
[47] S.R. Ghazali, K. Kubulat, M.I.N. Isa, A.S. Samsudin, W.M. Khairul, Contribution of methyl substituent on the conductivity properties and behaviour of CMC-alkoxy thiourea polymer electrolyte, Mol. Cryst. Liq. Cryst. 604 (1) (2014) 126.
[48] A. Saeed, M. Bolte, M.F. Erben, H. Pérez, Intermolecular interactions in crystalline 1-(adamantane-1-carbonyl)-3-substituted thioureas with Hirshfeld surface analysis, CrystEngComm 17 (39) (2015) 7551–7563.
[49] H.M. Abosadiya, S.A. Hasbullah, B.M. Yamin, Synthesis, X-ray, NMR, FT-IR, UV/vis, DFT and TD-DFT studies of N-(4-chlorobutanoyl)-N′-(2-, 3- and 4-methylphenyl)thiourea derivatives, Spectrochim. Acta. A. 144 (2015) 115.
[50] N.B. Arslan, C. Kazak, F. Aydin, N-(4-Nitrobenzoyl)-N′-(1,5-dimethyl-3-oxo-2-phenyl-1H-3(2H)-pyrazolyl)-thiourea hydrate: synthesis, spectroscopic characterization, X-ray structure and DFT studies, Spectrochim. Acta. A. 89 (2015) 30–38.
[51] D. Dang, P. Zhou, Q. Peng, K. He, H. Jiang, P. Yang, T. Hua, W. Yafei, L. Yu, L. Gangtie, W. Zhu, Improved photovoltaic performance of two-dimensional low band-gap conjugated polymers with thieno[3,2-b]thiophene and diketopyrrolopyrrole units by altering pendent position of conjugated side chain, Dyes. Pigments 109 (2014) 6–12.
[52] F. Tavoli, N. Alizadeh, Optical ammonia gas sensor based on nanostructure dye-doped polypyrrole, Sens. Actuat. B Chem. 176 (2013) 761.